Journal of Materials Chemistry A

Anion Conducting Multiblock Copolymers with Multiple Head-groups

Journal:	*Journal of Materials Chemistry A*
Manuscript ID	TA-ART-01-2018-000753.R2
Article Type:	Paper
Date Submitted by the Author:	14-Mar-2018
Complete List of Authors:	Liu, Lisha; Georgia Institute of Technology, Materials Science and Engineering Huang, Garrett; Georgia Institute of Technology, Chemical and Biomolecular Engineering Kohl, Paul; Georgia Institute of Technology, Department of Chemical and Biomolecular Engineering

Anion Conducting Multiblock Copolymers with Multiple Head-groups

Lisha Liu[1], Garrett Huang[2], and Paul A. Kohl[2*]

1. School of Materials Science and Engineering
2. School of Chemical and Biomolecular Engineering

Georgia Institute of technology

Atlanta, GA 30332-0100

[*]Corresponding author. Email address: kohl@gatech.edu

Abstract

Multiblock copoly(arylene ether)s with 1, 2, 3 and 4 alkyl chain tethered quaternary ammonium head-groups on each hydrophilic repeat unit were synthesized via polycondesation, Friedel-Crafts, and reduction reactions. The effect of the number of ionic groups on the ion exchange capacity (IEC), morphology and properties of the anion exchange membranes were investigated. As the ionic group density increased, both the ionic conductivity and water uptake of the membranes increased. The 3-tether membrane formed the most efficient ionic channels as determined by the highest ionic conductivity/IEC. The 2, 3, and 4-tether (per hydrophilic repeat unit) membranes had 9 to 10 bound waters of hydration per ionic group pair, however, the amount of unbound, freezable waters increased with the number of ion pairs per polymer repeat unit. The unbound, freezable water was unproductive and led to lower ionic conductivity/IEC ratio, such as in the 4-tether membrane. The optimum membrane had three head-groups per hydrophilic repeat unit (X_3Y_5-3): 130.6 mS/cm ionic conductivity at 80^{o}C, 58.3% water uptake, IEC of 1.83 meq/g. All the membranes showed acceptable thermal stability and alkaline stability in 1 M KOH at 60^{o}C for 1000 h. As the number of head-groups per hydrophilic repeat unit increased, the mechanical strength of the membranes decreased.

Introduction

The development of high performance anion exchange membranes (AEMs) for electrochemical devices (*i.e.* fuel cells, electrolyzers, redox flow battery, etc.) has attracted attention due to their potential advantages over cation exchange membranes.[1-6] Alkaline conditions can have more facile electrochemical kinetics and enable the use of low-cost, non-precious metal catalysts. However, anion conducting membranes can have lower ionic conductivity than cation conducting membranes and the chemical stability at high pH and high temperature condition can be challenging.[2,7-11] Recently, Mohanty and Dang have demonstrated good ionic conductivity and excellent chemical stability of AEMs.[12,13] It is of interest to explore how much improvement in conductivity and other properties can be achieved with block copolymers and high ion exchange capacity (IEC).

High ionic conductivity (*i.e.* greater than 100 mS/cm at 80^{o}C) is desired for fuel cell and electrolyzer applications. Ionic conductivity is a function of the number of ions (i.e. ion exchange capacity (IEC)) and the mobility of the ions within the membrane. The low ion mobility in some AEMs can be due to (i) inherently lower ion mobility of OH^- compared to H^+, and (ii) low ionization of ammonium hydroxide groups.[2] Ion mobility can be improved by forming efficient ion conductive channels in the membranes. One method of constructing efficient ionic channels is through phase segregation within block copolymers and graft polymers where ionic head-groups are concentrated in the hydrophilic domains. Park et al.[14] reported that multiblock copolymers have higher ionic conductivity and lower water uptake than their corresponding random copolymers with the same IEC.

The second contributing factor in improving conductivity is to increase the density of charge carriers in the membrane, as characterized by the IEC. However, increasing the IEC has

often led to high water uptake which can swell the AEM and decrease its mechanical toughness by flooding the ionic channels with water. It has been found that some water is necessary within the AEM for water hydration while excess, unbound water is unproductive and causes channel flooding.[14] Thus, there is an optimum water concentration within an AEM.

There are different strategies and configurations for attaching the fixed cation to the polymer backbone.[15] Tethering the cations via long, pendant alkyl spacers has been shown to be effective in improving microphase separation, hydroxide ion conductivity, and alkaline stability.[15-19] The polymer becomes a comb-shaped with the addition of long alkyl side chains. A grafted polymer configuration also facilitates the nanophase separation between the conductive domains and nonconductive domains. Jannasch et al.[20] compared the morphology and properties of a series of poly(phenylene oxide)s with cationic alkyl side chains of different lengths and configurations. It was found that the flexible spacer units helped form efficient ionic phase separation. The resulting membrane with long alkyl spacers had high OH^- conductivity, exceeding 100 mS/cm at 80^{o}C. Previous concerns with membrane degradation via the Hofmann elimination reaction with quaternary ammonium (QA) groups bound to long alkyl chains have been shown to be unfounded. Mohanty et al.[21] reported that degradation via β-Hofmann elimination was a minor factor for alkyl-tethered QAs. The S_N2 degradation pathway was a more important degradation route in their accelerated aging experiments. Several studies reported that long, alkyl chain tethered QA groups showed surprisingly good alkaline stability. Hibbs[22] reported that membranes with trimethylammonium cations attached by a hexamethylene spacer showed better stability than the membranes with benzyl trimethylammonium cations in 4 M KOH at 90^{o}C. In small molecule studies, Bae et al.[23] reported that QA groups attached via a six-carbon alkyl spacer were the most stable under alkaline conditions. It appears that the electron

density around the beta hydrogens in long alkyl tethers can inhibit Hofmann elimination reaction.[24] In addition, the steric shielding in the β-positions may also play a role in the stability of long alkyl chains.[25]

In this study, the density of fixed, tethered cations within the AEM is systematically varied so as to see the overall effect ion density on (i) conducting channel size, (ii) channel efficiency (as measured by conductivity/IEC), and (iii) type of water in the polymer (productive or non-productive water). A multiblock copoly(arylene ether)s (mPEs) backbone was chosen because it is a unique structure where the IEC can be systematically varied in a highly controlled fashion by attaching cationic head-groups via long alkyl chain tethers one-at-a-time. The goal is to explore the relationship between the morphology and properties of the AEMs with different IECs. The number of ionic head-groups on the polymer backbone can be precisely controlled by use of the unique characteristics of the Friedel-Crafts tether-addition reaction. Each tether was successively attached to each hydrophilic block. Specifically, 1, 2, 3, and 4 ionic groups were attached on each repeat unit in the hydrophilic block of the copolymer. It is noted that the 4-tether mPE membrane had an exceptionally high IEC value within the hydrophilic blocks, 3.13 meq/g, as compared to previous AEMs. The size of the ion conductive channels, ionic conductivity, water uptake, and number of bound and unbound water molecules in the membranes were also evaluated.

Experimental section

Materials: N,N'-dimethylacetamide (DMAc) was obtained from Alfa Aesar and dried by vacuum distillation at 130°C over CaH_2. Decafluorobiphenyl (DFBP), 4,4'-(hexafluoroisopropylidene)diphenol (HFBPA), 6-bromohexanoyl chloride, $AlCl_3$, 1,2-dichloroethane, triethylsilane, and trifluoroacetic acid were obtained from Alfa Aesar. 4,4'-(9-

fluorenylidene)diphenol (BPFL) was obtained from TCI Co. Ltd. Potassium carbonate (K_2CO_3) and dichloromethane (DCM) were purchased from BDH chemicals. All chemicals were used as received unless otherwise noted.

Synthesis of hydrophobic and hydrophilic oligomers: The synthetic procedure for the hydrophobic oligomer with three repeat units (x=3) is as follows: DFBP (1.67 g, 5 mmol) and HFBPA (1.68 g, 5 mmol) were dissolved in 20 mL DMAc in a 100 mL three-neck round bottom flask with a condenser under N_2 atmosphere at room temperature. K_2CO_3 (1.66 g, 12 mmol) was added to the solution and then the mixture was heated to 80˚C for 1 hr. DFBP (0.5 g) was added to the mixture and allowed to react at 40˚C for 4 h to ensure that all the oligomers were hydroxyl-terminated. The viscous solution was poured into deionized water to precipitate the product. The white solid was isolated by filtration, washed three times with deionized water and dried overnight at 80^{o}C in a vacuum oven. Hydrophobic oligomers with a different number of repeat units were synthesized by controlling the reaction time.

Fluoro-terminated hydrophilic oligomer with five repeat units (y=5) was synthesized via a similar procedure. BPFL (1.75 g, 5 mmol) and DFBP (1.67 g, 5 mmol) were dissolved in 20 mL DMAc under N_2 atmosphere. K_2CO_3 (1.66 g, 12 mmol) was added to the solution and the mixture was reacted at 80 □ for 2 h. BPFL (0.6 g) was added to the mixture and reacted at 40^{o}C for 4 h. After precipitation, filtration and drying, a white solid was yielded. Similarly, hydrophilic oligomers with different amount of repeat units were obtained by varying reaction time.

Synthesis of multiblock copoly(arylene ether)s (mPEs): The hydrophobic oligomer (1.11 g, 0.5 mmol, x = 3) and hydrophilic oligomer (1.78 g, 0.5 mmol, y = 5) were dissolved in 20 mL DMAc at room temperature under N_2. K_2CO_3 (0.15 g, 1.1 mmol) was added to the solution and

the mixture was reacted at 80°C for 4 h. The viscous solution was poured into deionized water and white solid was precipitated out. The product was filtrated, washed with deionized water and dried overnight at 80°C in a vacuum oven.

Synthesis of 1-tether BrKC6-mPEs: Multiblock copolymer mPE-X_3Y_5 (1.16 g, 1 mmol hydrophilic repeat units) was dissolved in 20 mL DCM in a flask under nitrogen atmosphere. The flask was chilled in an ice bath. 6-bromohexanoyl chloride (0.6 mL, 4 mmol) and $AlCl_3$ (0.54 g, 4 mmol) were added to the solution and warmed to room temperature. The mixture was reacted for 5 h at room temperature. The solution was poured into 200 mL deionized water and heated to 60°C to evaporate the solvent. The product was dissolved in DCM and precipitated in deionized water three times to obtain a purified light yellow solid.

Synthesis of 1-tether BrC6-mPEs: BrKC6-mPE-X_3Y_5 (1.32 g, 1 mmol hydrophilic repeat units) was dissolved in 20 mL 1,2-dichloroethane in a three-neck round bottom flask with a condenser at room temperature under nitrogen. Trifluoroacetic acid (3.8 mL, 50 mmol) and triethylsilane (0.8 mL, 5 mmol) were added to the solution. The solution was heated to reflux for 24 h. After cooling to room temperature, it was poured into a NaOH solution (2 g NaOH, 200 mL deionized water). The mixture was heated to 80°C to evaporate the solvent. The product was isolated by filtration. The product was dissolved in DCE and precipitated in deionized water three times producing a white solid product.

Synthesis of multi-tether BrKC6-mPEs and BrC6-mPEs: Multi-tether BrKC6-mPEs and BrC6-mPEs were synthesized via repeated Friedel-Crafts reaction and reduction reaction described in the previous steps.

Membrane casting, quaternization and ion exchange: BrC6-mPEs (0.20 g) was dissolved in 5 mL 1,2-dichloroethane and the resulting solution was filtered through a 0.45 μm poly(tetrafluoroethylene) (PTFE) membrane syringe filter into a 4-cm diameter aluminum dish. The solvent was evaporated in a tube furnace at 40^{o}C under nitrogen for 18 h. The free-standing membrane was about 40 μm thick.

The membrane was quaternized as follows: immersion in 45 wt % trimethylamine aqueous solution at room temperature for 48 h. After being removed from the solution, the quaternized membrane with a bromide counter ion was washed with deionized water three times. The membrane was soaked in 1 M KOH solution under nitrogen for 24 h to exchange the bromide ions for hydroxide ions. After being washed with deionized water three times, the membrane was stored in deionized water.

Nuclear magnetic resonance (NMR) spectra and gel permeation chromatography (GPC): The chemical structure of the oligomers and polymers were analyzed by a variety of NMR techniques, including one-dimensional ^{1}H NMR and ^{19}F NMR obtained with a Varian Mercury Vx 400 MHz spectrometer. Chloroform-*d* was used as the NMR solvent. Quantitative ^{19}F NMR spectra were collected at 376.273 MHz with a 12.5 s relaxation delay.

The molecular weight of the polymers was determined by gel permeation chromatography (GPC) (Shimadzu) equipped with an LC-20 AD HPLC pump and a refractive index detector (RID-10 A, 120 V). Tetrahydrofuran (THF) was used as the eluent with at a flow rate of 1.0 mL/min at 35^{o}C. The molecular weight was measured against a polystyrene standard.

Ionic conductivity: The ionic resistance of the membranes was measured with a four-probe, in-plane electrochemical impedance spectrometer over the frequency range from 1 Hz to 1

MHz with a PAR 2273 potentiostat. All samples were tested in HPLC-grade water under nitrogen to minimize the effect of CO_2. The samples were equilibrated for 30 min prior to measurement. The in-plane ionic conductivity was calculated using Equation 1.

$$\sigma = \frac{L}{WTR} \quad (1)$$

In Eq. 1, σ is the ionic conductivity in S/cm, L is the length between sensing electrodes in cm, W and T are the width and thickness of the membrane in cm, respectively, and R is the resistance measured in ohms.

Ion exchange capacity (IEC), water uptake (WU), hydration number (λ), number of freezable water (Nfree) and bound, non-freezable water (Nbound) molecules: The ion exchange capacity was calculated using 100% quaternization conversion of the alkyl bromide from NMR analysis as described in our previous work. The IEC was calculated by Equation 2.

$$IEC = \frac{N_{tethery}}{M_b} \quad (2)$$

The water uptake of the membranes was calculated by Equation 3.

$$\mathrm{WU}(\%) = \frac{M_w - M_d}{M_d} \times 100 \quad (3)$$

In Eq. 2, M_d is the dry mass of the membranes measured after being dried in vacuum for 24 hr and M_w is the wet mass of the membranes without surface water. Both dry and wet membranes were in the OH^- form and measured at room temperature. The number of water molecules per ionic group, hydration number λ, was calculated using Equation 4.

$$\lambda = \frac{1000 \times WU\%}{IEC \times 18} \quad (4)$$

The number of freezable water (N_{free}) and bound water (or non-freezable water) (N_{bound}) were determined by differential scanning calorimetry (DSC). DSC measurements were carried out on a DSC Q200 (TA Instruments). The membrane samples were fully-hydrated by soaking in deionized water at least for one week. After the water on the membrane surface was wiped off, a 3 to 5 mg sample was quickly sealed in an aluminum pan. The sample was cooled to -50^{o}C and heated to room temperature at a rate of 5^{o}C/min under N_2 (20 mL/min). The quantity of freezable and non-freezable water was determined by Equations 5 to 7.[26-28]

$$N_{free} = \frac{M_{free}}{M_{tot}} \times \lambda \quad (5)$$

M_{free} is the mass of freezable water and M_{tot} is the total mass of water absorbed in the membrane. The weight fraction of freezable water was calculated by Equation 6.

$$\frac{M_{free}}{M_{tot}} = \frac{H_f/H_{ice}}{(M_W - M_d)/M_w} \quad (6)$$

H_f is enthalpy obtained by the integration of the DSC freezing peak and H_{ice} is enthalpy of fusion for water, corrected for the subzero freezing point according to Equation 7.

$$H_{ice} = H_{ice}^{o} - \Delta C_p \Delta T_f \quad (7)$$

ΔC_p is the difference between the specific heat capacity of liquid water and ice. ΔT_f is the freezing point depression.

Morphological characterization: Small angle X-ray scattering (SAXS) was used to analyze the morphology of AEMs. Dry membranes in Br^- form were tested in a Malvern Panalytical Empyrean XRD (Netherlands) with a Pixel 3D detector. The scattering experiments were performed using Cu Kα radiation with a wavelength (l) of 1.542 □ generated within a high

brilliance micro focus sealed tube with shaped multilayer optics operating at 45 kV and 40 mA. The wave vector (q) was calculated as:

$$q = \frac{4\pi}{l \sin 2\theta} \quad (8)$$

where 2θ is the scattering angle. The characteristic separation length, or interdomain spacing (d) (i.e. the Bragg spacing) was calculated, Equation 9.

$$d = \frac{2\pi}{q} \quad (9)$$

Transmission electron microscopy (TEM) was also used to analyze the morphology of the membranes. TEM was performed on a JEOL JEM-1400 Transmission Electron Microscope. The membranes in bromide ion form were stained with osmium tetroxide at room temperature prior to examination. The stained membranes were embedded within an epoxy resin, sectioned into approximately 50 nm thick samples with a Leica UC6rt Ultramicrotome, and placed on copper grids for observation.

Thermal stability: Thermal stability of the hydroxide form of the membranes was analyzed by thermogravimetric analysis (TGA) on a TA Instruments Q50 analyzer. The thermal degradation was evaluated at a heating rate of 5^{o}C/min up to 800^{o}C in nitrogen.

Mechanical properties: The stress-strain relationship was investigated by dynamic mechanical analysis (DMA) using TA Instruments Q800 with controlled force mode. Rectangular membrane samples were fully hydrated and tested using tension clamps after removing surface water at 100% relative humidity. The experimental parameters were set as: preload force 0.05 N, isothermal at 30^{o}C, soak time 1 min, force ramp rate 0.5 N/min and upper force limit up to 18 N.

Alkaline stability: The alkaline stability of the membranes was evaluated by soaking the OH^- form membranes into 1 M NaOH in a Teflon lined Parr reactor at 60°C for up to 1000 h to measure the changes in ionic conductivity. Before measurement, each membrane was thoroughly washed with deionized water. The ionic conductivity was determined in HPLC-grade water at room temperature.

Results and discussion

Synthesis and structural analysis of 1, 2, 3 or 4-tether multiblock copoly(arylene ether)s

The structure of the 1, 2, 3 and 4-tether multiblock copoly(arylene ether)s (mPEs) are shown in Figure 1. All the samples had the same multiblock backbone structure (X_3Y_5), synthesized via polymer condensation reaction of hydrophobic oligomers (x = 3 repeat units) and hydrophilic oligomers (y = 5 repeat units), as previously described.[17] The molecular weight of the polymer backbone, mPE-X_3Y_5, measured by GPC was 67.2 kDa. The ionic head groups with long tethers were attached to the multiblock copolymer mPEs backbone via a Friedel-Crafts reaction with 6-bromohexanoyl chloride and $AlCl_3$, followed by chemical reduction to reduce the tether's ketone group to an alkyl. The reactivity of the fluorene aromatic rings is low due to the electron-withdrawing nature of the ketone group on the tether. Thus, only one head-group tether could be attached on each hydrophilic repeat unit with each Friedel-Crafts reaction, even though 6-bromohexanoyl chloride was used in excess and multiple sites were available for tether attachment. However, after the reduction of the ketone group to an alkyl, the aromatic group ring regained its reactivity, and an additional tether could be attached. This one-at-a-time characteristic of the tether attachment reaction has been used to precisely control the number of the ionic head-groups attached to each hydrophilic repeat unit of the polymer backbone. Multi-

tether, multiblock copolymers were synthesized via repeated Friedel-Crafts followed by reduction reactions. From our previous structural analysis of ^{1}H NMR spectra[65], the first two tethers were attached at f position, as shown in Figure 2.

The third and fourth tether were attached at position h'' on the fluorene aromatic ring. This was shown by integration area of the proton peak h'' at 7.70 ppm. The h'' peak was reduced to half of its amount after the third tether was attached, as shown in Figure 2(a). The singlet peak at 7.22 ppm corresponds to the aromatic protons at position e''. The overlapping singlet and doublet peak at 7.10 ppm was attributed to the g'' and g''' protons. The integration areas of these two peaks were twice that of peak h'', which is another piece of evidence showing attachment of the third tether at position h''. The 1:2 ratio of the peak areas for the protons at positions i' and p confirm the successful attachment of the third tether. The 1:6 ratio of the peak area for the proton at h'' on the fluorene aromatic ring and the overlapping peaks n and n', attributed to the methylene protons adjacent to the bromide groups, is another piece of evidence for the third tether attachment. After the ketone group of the third tether was reduced, the i' peak disappeared and the peak ratio for the protons at n and p became 1:1, as shown in Figure 2(b). The attachment of the fourth tether was shown by the disappearance of the h'' peak and 1:3 peak ratio of protons i' and p, shown in Figure 3(a). After reduction of the ketone group, the i' peak disappeared and the peak ratio of protons at n and p changed back to 1:1, as in Figure 3(b).

Morphology

Small angle X-ray scattering (SAXS) measurements were performed to investigate the microstructure of the membranes with a different number of alkyl chains terminated with quaternary ammonium head-groups. The polymers were tested dry with an iodide counter ion.

The average separation length between inhomogeneities in the membrane, or interdomain spacing, d, was calculated from the position of the scattering maximum (q_{max}) via Braggs law. The multiblock AEM copolymers with 1, 2, 3, and 4 ionic head-groups on each hydrophilic repeat unit showed scattering peaks with q_{max} values, 0.140, 0.112, 0.107 and 0.105 nm^{-1}, respectively, as shown in Figure 4. This corresponds to interdomain spacing, d, of 44.8, 56.1, 58.7, and 59.8 nm, respectively, as summarized in Table 1. This separation magnitude suggests that the scattering was due to phase segregation of the multiblock copolymer structure stemmed from the thermodynamic incompatibility of the hydrophilic/hydrophobic blocks, rather than simply the formation of ion clusters in a random polymer which would have only showed a small value for d.[15] The interdomain spacing of the membranes was influenced by the length of the hydrophobic and hydrophilic blocks, the length of head-group tethers, and the ionic group density. A larger value of the interdomain spacing usually suggests a larger size of the ion conductive channel.[29,30] These results show that an increase in the number of the alkyl chain tethered quaternary ammonium groups results in an increase in the interdomain spacing. The large difference in the d values for the 1 and 2-tether polymers indicates that the density of tethered ionic groups had a significant influence on the channel size. However, this influence became less dramatic with additional tethers.

TEM images were obtained to examine the morphology of the membranes, as shown in Figure 5. Phase separation is observed in the images of 2, 3, and 4-tether membranes in bromide form. The dark regions correspond to hydrophilic domains with bromide counter ions and the bright regions correspond to hydrophobic domains.[30] Analysis was performed in the bromide form rather than the hydroxide form because drying the hydroxide membrane concentrates the hydroxide to a point where inadvertent degradation could occur. The hydrophilic domains appear

to form contiguous ion conductive channels. The average size of the ion conductive channels of 2, 3, 4-tether samples were about 18, 28, and 38 nm, respectively. The TEM images showed that more continuous and larger size ion conductive channels were formed in the membrane with an increase in the number of ionic groups (i.e. ion concentration in the hydrophilic blocks). The formation of these ion conducting channels has a great impact on the ionic conductivity and water uptake of the membranes.

Ion exchange capacity (IEC) and ionic conductivity

As shown in Table 1, the overall IEC was calculated for the multiblock copolymer. The local IEC was calculated corresponding to the density of ionic groups within only the hydrophilic blocks. It is can be seen that both the overall IEC and local IEC increased with the number of tethers attached to the hydrophilic repeat units. The local IEC of 4-tether mPE membrane reached 3.13 meq/g, which is large compared with other AEM membranes reported in the literature.

Figure 6 shows the hydroxide conductivity of the membranes at 20, 40, 60 and 80^{o}C. The ionic conductivity increases with temperature and follows an Arrhenius relationship. The slope of the Arrhenius plot corresponds to the activation energy for the ionic conductivity, which was in the range of 17 to 22 kJ/mol. The ionic conductivity increased with the increasing of IEC, resulting from the increase of the number of ionic groups. This observation was also demonstrated in other studies.[31] Membranes with a greater number of ionic groups form larger ion conductive channels, which facilitates ion transport in the membrane, resulting in higher ionic conductivity. The ratio of the ionic conductivity to IEC was calculated to evaluate the effectiveness of the ionic groups, as shown in Table 1. The ionic conductivity/IEC value

increased with the ionic group concentration, however, it reached a maximum with the 3-tether membrane, suggesting that this structure demonstrates the highest ionic group efficiency. The efficiency decreased as the fourth tether was attached, even though the 4-tether membrane showed the highest absolute ionic conductivity.

Water uptake (WU), hydration number (λ), number of freezable water molecules (N_{free}) and bound, non-freezable water molecules (N_{bound})

A critical amount of water is necessary for ion hydration and conduction in the membranes. However, excess water, especially in the form of free-water, in the membranes results in membrane swelling, lower mechanical toughness, and flooding of the ion conductive channels. The phase segregation of block copolymers and the partial fluorination of the backbone structure, which introduces great hydrophobicity, can effectively control the water uptake at a relatively low level. The water uptake in the membranes with 1, 2, 3 and 4 alkyl side chain tethers in hydroxide ion form at room temperature is shown in Table 1. The water uptake increased with the number of ionic groups (or IEC). The 2-tether membrane had an ionic conductivity of 86.1 mS/cm at 80^{o}C with only 26% water uptake. The 3-tether membrane showed 130.6 mS/cm ionic conductivity at 80^{o}C with 50% water uptake which is relative low compared to membranes with very high ionic conductivity. Though the 4-tether membrane also showed a very high ionic conductivity, the water uptake was also high, which leads to excess swelling. This is due to the relatively large size of the ion conductive channels and high density of head groups.

The hydration number (λ) is the number of water molecules per ionic head-group (cation/anion pair). Excess water in the form of free (unbound) water is not desirable or

productive for ion conduction. The hydration number also increased somewhat as the number of ionic groups in hydrophilic blocks, as shown in Table 1. The water molecules in the membrane can be divided into two states: freezable water molecules slightly associated with ion exchange groups, and non-freezable (bound) water molecules bound to an ion or polymer matrix. The number of freezable (N_{free}) and non-freezable (N_{bound}) water molecules was investigated by DSC and summarized in Table 1. The freezable water will show a characteristic freezing peak at temperatures below at 0^{o}C, while non-freezable water will show no peaks in DSC thermogram. Our previous work showed that the two-tether multiblock copolymer mPEs membranes had a similar amount of bound water molecules: 9 to 10, per ionic pair, or 4.5 to 5, per cation or anion.[65] In this work, the 2-tether sample showed a similar result. In addition, the number of bound water molecules for the 3 and 4-tether membranes was also in this range. Therefore, the increase of the number of head-groups (> 2 tethers) had little effect on the increase of the number of bound water molecules per head group. In contrast, the increase in density of head groups greatly affected the freezable water content in the membranes. 1 and 2-tether membrane showed very little freezable water, while 3 and 4-tether polymers had a large amount of freezable water. This explained the high water uptake of 3 and 4-tether sample. It also suggests that the ion conductive channels must be large enough for the bound water and have enough room for the freezable water. The 4-tether sample had a large amount of freezable water, resulting in 82.5% water uptake and lower ionic conductivity/IEC.

Alkaline stability

It was reported previously[17] that the 1 or 2-tether mPEs membranes with long tether attached quaternary trimethyl ammonium showed acceptable alkaline stability in strong base solutions at 60^{o}C. There was only 1 to 3% drop in ionic conductivity after soaking in 1M NaOH

solution at 60°C for 1000 h. The 3-tether and 4-tether mPEs membranes were tested at the same conditions as the 1 and 2-tether samples. The results show that the ionic conductivity of the X_3Y_5-3 and X_3Y_5-4 membrane reduced by only 1.4 and 1.9%, respectively, and are very similar to the 2-tether sample, Figure 7. The alkaline stability is not undermined with more ionic head-groups attached. Therefore, it can be concluded that the long alkyl tether for quaternary trimethylammonium ionic exchange groups have acceptable alkaline stability compared to many other AEM materials with benzyl trimethylammonium groups.

Thermal stability

Figure 8 shows the thermal degradation behavior of mPEs membranes with a different number of tethers in the hydroxide form via TGA. Regardless of the number of the tethers, these membranes showed similar thermal degradation pattern. The initial weight loss below 100˚C was due to the evaporation of bound and unbound water in the membrane. The mPEs membranes followed a three-stage weight loss. From 180°C to 220°C the weight loss was due to the degradation of the quaternary ammonium groups. From 220°C to 400°C, it was due to the degradation of the long alkyl side chains. Above 400°C, polymer backbone degraded. Therefore, the membranes are thermally stable enough under the common operation temperature of fuel cells or electrolyzers (*i.e.* below 100°C).

Mechanical properties

Good mechanical stability of the membrane is indispensable for the fabrication of the membrane electrode assembly and the operation of electrochemical devices. Devices often have a pressure difference between the two sides of the membrane. The mechanical properties were

obtained from stress-strain curve of mPEs membranes tested from DMA, as summarized in Table 2.

The values of tensile strength, Young's modulus, and elongation at break show that the membranes had adequate mechanical strength for many applications. It was observed that the tensile strength and the elongation at break decreased with the increase in the number of ionic groups. This was likely due to the increase of water content, which might act as a plasticizer in the membranes and disintegrate tightly arranged polymer chains. In addition, with the increase of the tether structure, the arrangement of polymer chains was further disrupted.

Conclusions

The effect of ionic concentration in hydrophilic block of multiblock copolymers on the morphology and properties of anion exchange membranes were systematically investigated in this work. The multiblock copolymer mPEs with 1, 2, 3 and 4 long alkyl chain tethered ionic groups on each repeat unit in hydrophilic block, resulting in different ion exchange capacity (IEC), were synthesized and compared. Only one head-group tether can be attached on each hydrophilic repeat unit at a time. Thus, the tether amount can be precisely controlled. As the ionic concentration increased, the ionic conductivity and water uptake of the membranes increased. This was due to the increase of the size of ion conductive channels. 3-tether membrane showed the highest ionic conductivity/IEC, which means that its ionic groups were most efficient for contributing to the ionic conductivity. In addition, the number of freezable and non-freezable water molecules were investigated. 2, 3, 4-tether membrane showed similar number of bound water, while the number of freezable water increased with the number of ionic groups. The excess freezable water led to high water uptake and low ionic conductivity/IEC ratio

(i.e. X_3Y_5-4). Therefore, X_3Y_5-3 showed the best properties, 130.6 mS/cm ionic conductivity at 80^{o}C and 58.3% water uptake, with an IEC of 1.83 meq/g. All of the membranes showed the same thermal and alkaline stability. As the number of ion groups increased, the mechanical strength of the membranes declined.

Acknowledgements

We gratefully acknowledge the financial support of the Army Research Laboratory (ARL), especially Dr. Deryn Chu, and the Advanced Research Projects Agency-Energy's (ARPA‐E) project from the Department of Energy, DE-AR0000769. We also acknowledge the valuable discussions with Dr. Chulsung Bae of Rensselaer Polytechnic Institute.

References

(1) Steele, B. C. H.; Heinzel, A. *Nature* **2001**, *414*, 345.

(2) Varcoe, J. R.; Atanassov, P.; Dekel, D. R.; Herring, A. M.; Hickner, M. A.; Kohl, P. A.; Kucernak, A. R.; Mustain, W. E.; Nijmeijer, K.; Scott, K.; Xu, T.; Zhuang, L. *Energy & Environmental Science* **2014**, *7*, 3135.

(3) Li, N.; Guiver, M. D. *Macromolecules* **2014**, *47*, 2175.

(4) Leng, Y.; Chen, G.; Mendoza, A. J.; Tighe, T. B.; Hickner, M. A.; Wang, C.-Y. *Journal of the American Chemical Society* **2012**, *134*, 9054.

(5) Zeng, K.; Zhang, D. *Progress in Energy and Combustion Science* **2010**, *36*, 307.

(6) Alotto, P.; Guarnieri, M.; Moro, F. *Renewable and Sustainable Energy Reviews* **2014**, *29*, 325.

(7) Hickner, M. A.; Herring, A. M.; Coughlin, E. B. *Journal of Polymer Science Part B: Polymer Physics* **2013**, *51*, 1727.

(8) Merle, G.; Wessling, M.; Nijmeijer, K. *Journal of Membrane Science* **2011**, *377*, 1.

(9) Couture, G.; Alaaeddine, A.; Boschet, F.; Ameduri, B. *Progress in Polymer Science* **2011**, *36*, 1521.

(10) Varcoe, J. R.; Slade, R. C. T. *Fuel Cells* **2005**, *5*, 187.

(11) Gottesfeld, S.; Dekel, D. R.; Page, M.; Bae, C.; Yan, Y.; Zelenay, P.; Kim, Y. S. *Journal of Power Sources* **2018**, *375*, 170.

(12) Mohanty, A. D.; Ryu, C. Y.; Kim, Y. S.; Bae, C. *Macromolecules* **2015**, *48*, 7085.

(13) Dang, H.-S.; Jannasch, P. *Journal of Materials Chemistry A* **2017**, *5*, 21965.

(14) Park, D.-Y.; Kohl, P. A.; Beckham, H. W. *The Journal of Physical Chemistry C* **2013**, *117*, 15468.

(15) Jannasch, P.; Weiber, E. A. *Macromolecular Chemistry and Physics* **2016**, *217*, 1108.

(16) Lin, C. X.; Wang, X. Q.; Hu, E. N.; Yang, Q.; Zhang, Q. G.; Zhu, A. M.; Liu, Q. L. *Journal of Membrane Science* **2017**, *541*, 358.

(17) Liu, L.; Ahlfield, J.; Tricker, A.; Chu, D.; Kohl, P. A. *Journal of Materials Chemistry A* **2016**, *4*, 16233.

(18) Ahlfield, J.; Huang, G.; Liu, L.; Kaburagi, Y.; Kim, Y.; Kohl, P. A. *Journal of The Electrochemical Society* **2017**, *164*, F1648.

(19) Pan, J.; Han, J.; Zhu, L.; Hickner, M. A. *Chemistry of Materials* **2017**, *29*, 5321.

(20) Dang, H.-S.; Jannasch, P. *Macromolecules* **2015**, *48*, 5742.

(21) Mohanty, A. D.; Tignor, S. E.; Sturgeon, M. R.; Long, H.; Pivovar, B. S.; Bae, C. *Journal of The Electrochemical Society* **2017**, *164*, F1279.

(22) Hibbs, M. R. *Journal of Polymer Science Part B: Polymer Physics* **2013**, *51*, 1736.

(23) Mohanty, A. D.; Bae, C. *Journal of Materials Chemistry A* **2014**, *2*, 17314.

(24) Komkova, E. N.; Stamatialis, D. F.; Strathmann, H.; Wessling, M. *Journal of Membrane Science* **2004**, *244*, 25.

(25) Tomoi, M.; Yamaguchi, K.; Ando, R.; Kantake, Y.; Aosaki, Y.; Kubota, H. *Journal of Applied Polymer Science* **1997**, *64*, 1161.

(26) Lue, S. J.; Shieh, S.-J. *Journal of Macromolecular Science, Part B* **2009**, *48*, 114.

(27) Mecheri, B.; Felice, V.; Zhang, Z.; D'Epifanio, A.; Licoccia, S.; Tavares, A. C. *The Journal of Physical Chemistry C* **2012**, *116*, 20820.

(28) Moster, A. L.; Mitchell, B. S. *Journal of Applied Polymer Science* **2009**, *113*, 243.

(29) Lin, C. X.; Wang, X. Q.; Li, L.; Liu, F. H.; Zhang, Q. G.; Zhu, A. M.; Liu, Q. L. *Journal of Power Sources* **2017**, *365*, 282.

(30) Pan, J.; Chen, C.; Li, Y.; Wang, L.; Tan, L.; Li, G.; Tang, X.; Xiao, L.; Lu, J.; Zhuang, L. *Energy & Environmental Science* **2014**, *7*, 354.

(31) Weiber, E. A.; Meis, D.; Jannasch, P. *Polymer Chemistry* **2015**, *6*, 1986.

Figure Captions

Figure 1. Structure of multiblock copoly(arylene ether)s with one tether "a", two tethers "a and b", three tethers "a, b and c", and four tethers "a, b, c and d".

Figure 1. ^{1}H NMR spectra of (a) 3-tether BrKC6-2BrC6-mPEs, and (b) 3-tether 3BrC6-mPEs.

Figure 2. ^{1}H NMR spectra of (a) 4-tether BrKC6-3BrC6-mPEs, and (b) 4-tether 4BrC6-mPEs.

Figure 3. SAXS data of mPE membranes with 1, 2, 3, and 4 long alkyl side chain tethered trimethyl quaternary ammoniums in iodide form. The data have been shifted vertically for clarity and the arrowheads indicate q_{max}.

Figure 4. TEM images of mPEs membranes in bromide form.

Figure 5. Arrhenius plot of ionic conductivity vs. inverse temperature.

Figure 6. Alkaline stability of the mPEs membranes with 2, 3, and 4 long alkyl side chain tethered ionic groups in 1 M NaOH solution at 60^{o}C. The data for the 2-tether membrane was previously published[17].

Figure 7. TGA curve of mPEs membranes with 1, 2, 3, and 4 long alkyl side chain tethered ionic groups under nitrogen atmosphere.

Table 1. Properties of the AEMs with 1, 2, 3, and 4 tethered ionic groups.

[a]Membrane	[b]Interdomain spacing, d (nm)	[c]Overall IEC (meq/g)	[d]Local IEC (meq/g)	[e]Ionic conductivity (mS/cm)		[f]σ/IEC	[g]Water uptake (%)	Hydration number, λ	N_{free}	N_{bound}
				25 □	80 □					
X_3Y_5-1	44.8	0.76	1.25	10.6	42.2	55.5	11.5	8.4	0.7	7.7
X_3Y_5-2	56.1	1.35	2.08	26.8	86.1	63.8	24.8	10.2	1.5	8.7
X_3Y_5-3	58.7	1.83	2.68	41.9	130.6	71.4	58.3	17.7	6.9	10.8
X_3Y_5-4	59.8	2.23	3.13	48.3	141.0	63.2	82.5	20.5	9.6	10.9

[a]1, 2, 3, 4: the number of head-group tethers on each hydrophilic repeat unit; X: hydrophobic block (3 repeat units); Y: hydrophilic block (5 repeat units); [b]Interdomain spacing d: average separation length between inhomogeneities (d) measured from SAXS; [c]Overall IEC: corresponding to the multiblock copolymer; [d]Local IEC: corresponding to the hydrophilic block; [e]Ionic conductivity: tested in hydroxide ion form; [f]σ/IEC: ratio of ionic conductivity at 80°C to IEC; [g]Water uptake: measured at room temperature in hydroxide ion form.

Table 2. Mechanical properties of mPEs membranes with 1, 2, 3, and 4 ionic groups.

Membrane	Tensile strength (Mpa)	Young's modulus (Gpa)	Elongation at break (%)
X_3Y_5-1	30.4	0.8	5.0
X_3Y_5-2	22.3	1.1	3.1
X_3Y_5-3	19.3	0.9	2.8
X_3Y_5-4	18.7	1.2	2.1

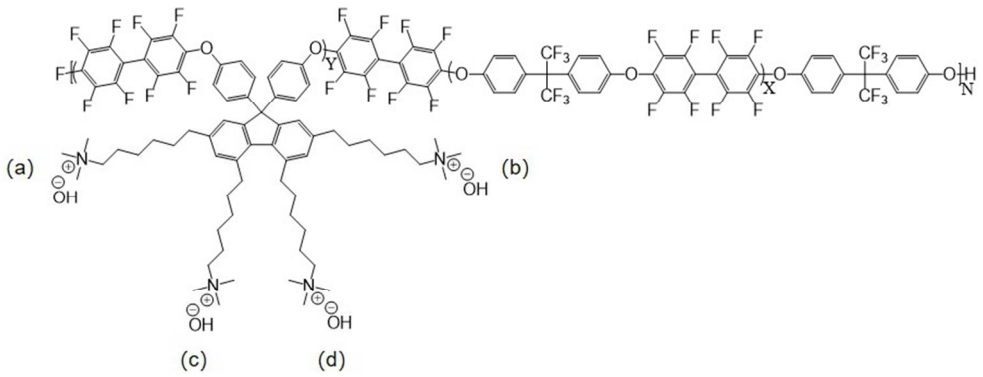

Figure 1. Structure of multiblock copoly(arylene ether)s with one tether "a", two tethers "a and b", three tethers "a, b and c", and four tethers "a, b, c and d".

243x92mm (96 x 96 DPI)

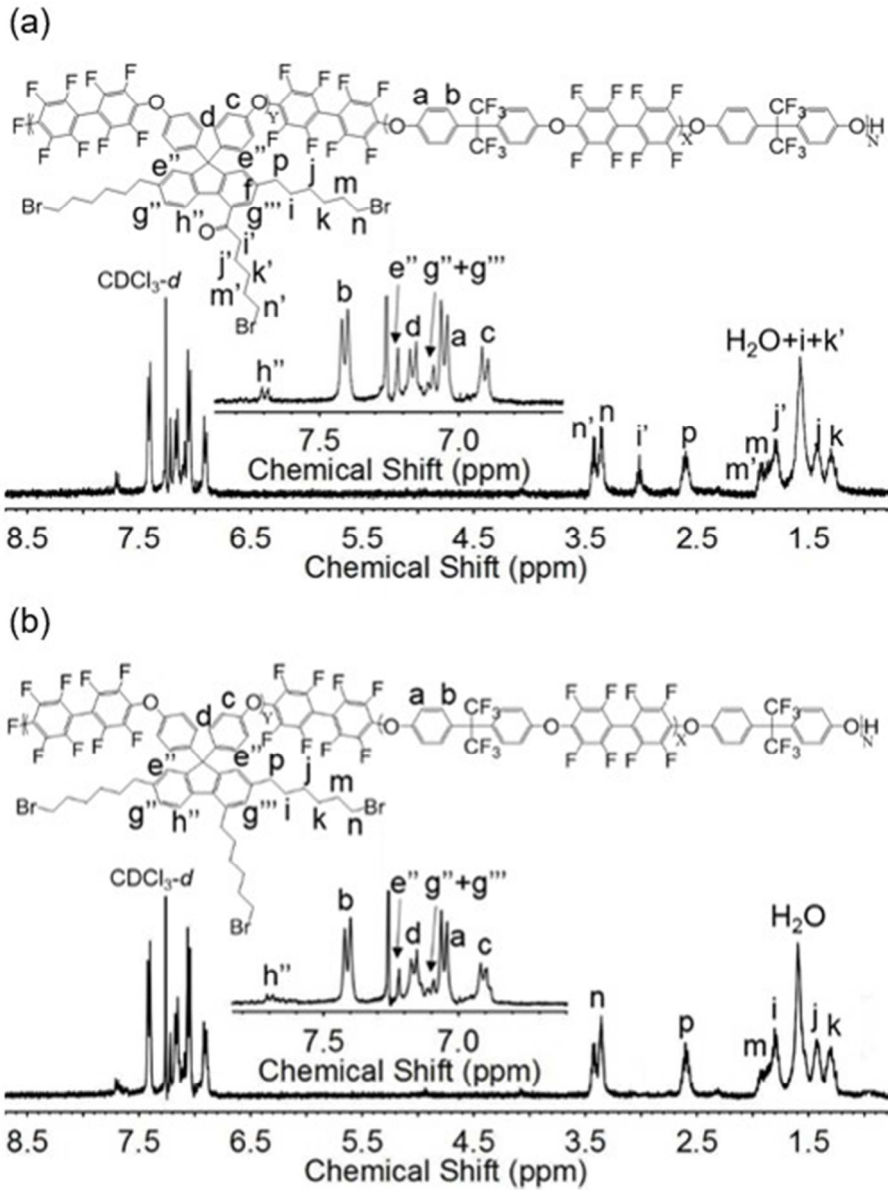

Figure 2. 1H NMR spectra of (a) 3-tether BrKC6-2BrC6-mPEs, and (b) 3-tether 3BrC6-mPEs.

132x175mm (96 x 96 DPI)

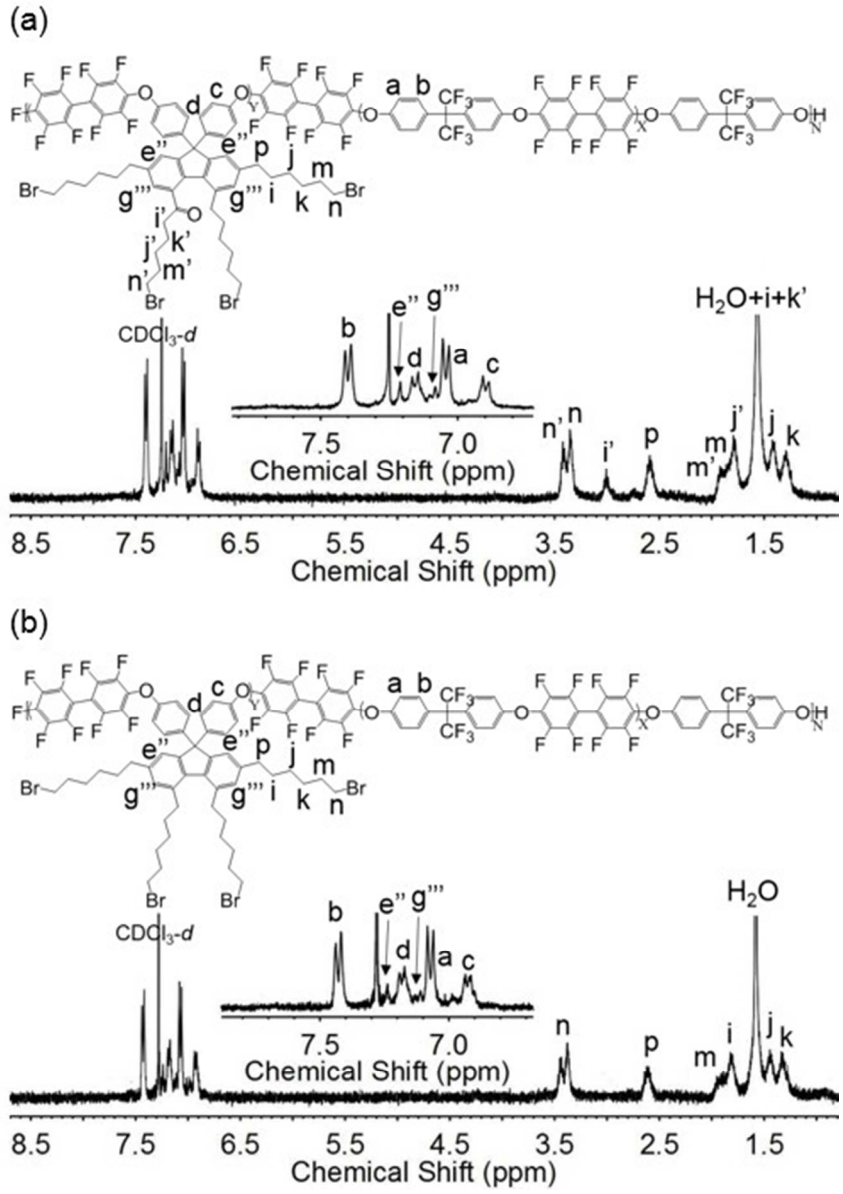

Figure 3. 1H NMR spectra of (a) 4-tether BrKC6-3BrC6-mPEs, and (b) 4-tether 4BrC6-mPEs.

133x187mm (96 x 96 DPI)

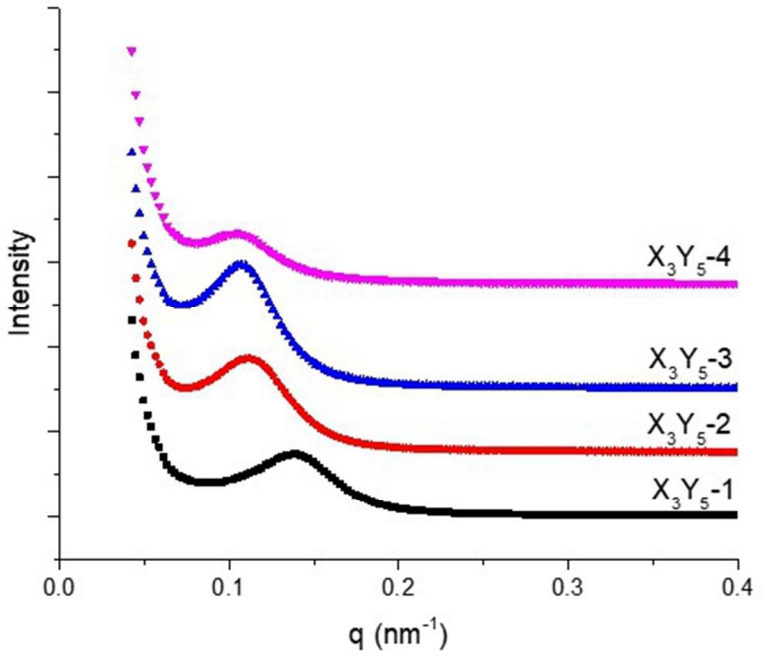

Figure 4. SAXS data of mPE membranes with 1, 2, 3, and 4 long alkyl side chain tethered trimethyl quaternary ammoniums in iodide form. The data have been shifted vertically for clarity and the arrowheads indicate qmax.

168x129mm (96 x 96 DPI)

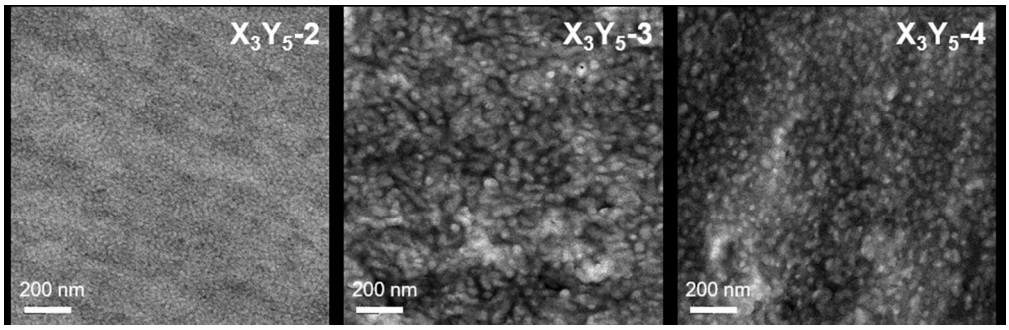

Figure 5. TEM images of mPEs membranes in bromide form.

254x81mm (96 x 96 DPI)

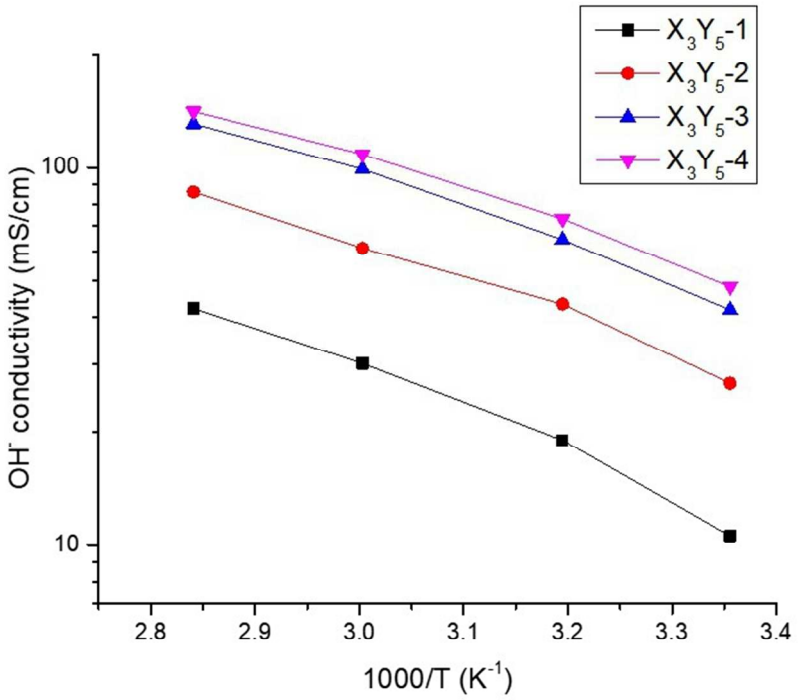

Figure 6. Arrhenius plot of ionic conductivity vs. inverse temperature.

224x173mm (96 x 96 DPI)

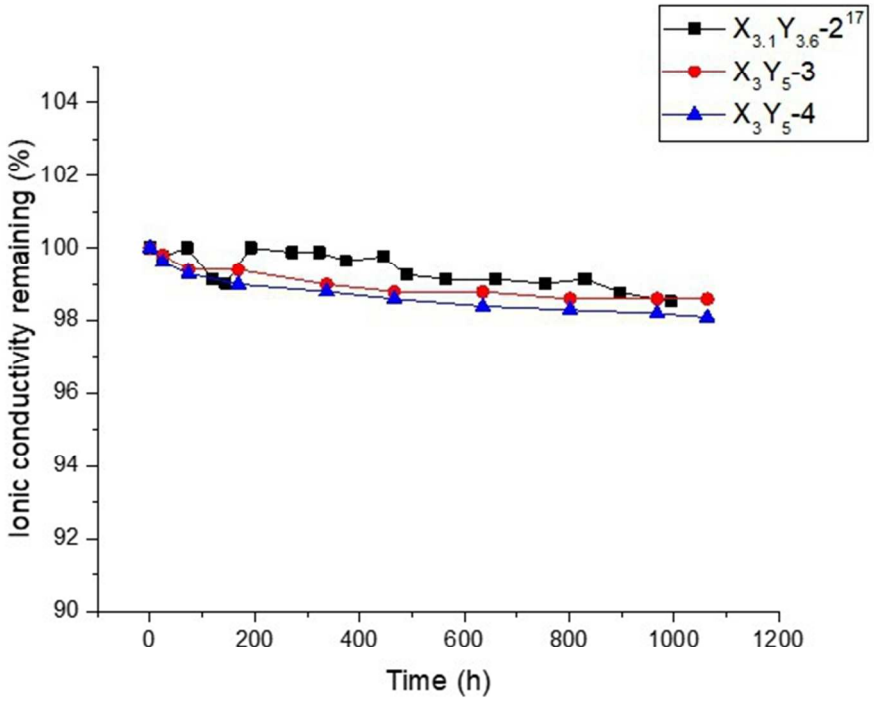

Alkaline stability of the mPEs membranes with 2, 3, and 4 long alkyl side chain tethered ionic groups in 1 M NaOH solution at 60oC. The data for the 2-tether membrane was previously published17.

170x130mm (96 x 96 DPI)

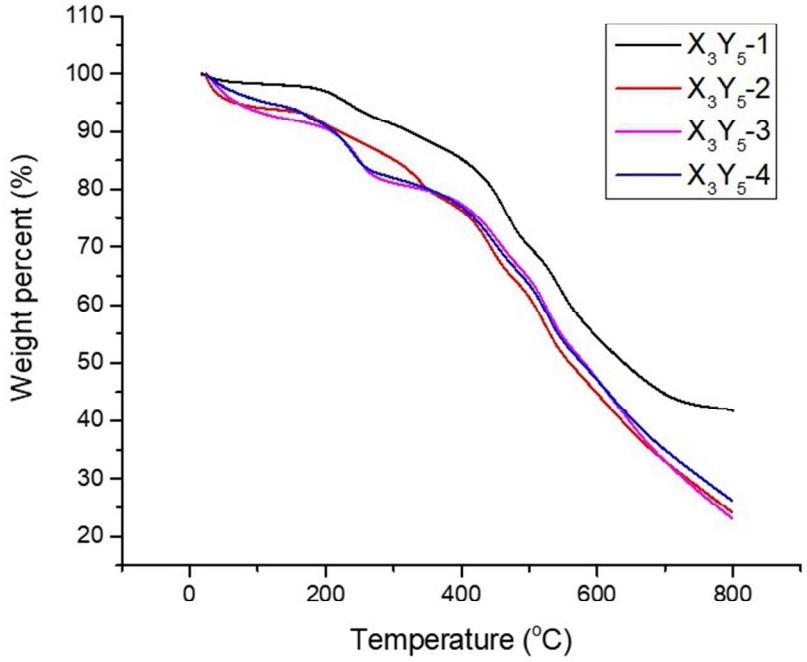

Figure 8. TGA curve of mPEs membranes with 1, 2, 3, and 4 long alkyl side chain tethered ionic groups under nitrogen atmosphere.

216x166mm (96 x 96 DPI)

Table of content entry

Multiblock copolymers with different number of head-group tethers were compared as AEMs for high ionic conductivity and good alkaline stability.